

A Systematic Investigation of Hydrogen-Bonding Effects on the ^{17}O , ^{14}N , and ^2H Nuclear Quadrupole Resonance Parameters of Anhydrous and Monohydrated Cytosine Crystalline Structures: A Density Functional Theory Study

Mahmoud Mirzaei, Fatemeh Elmi, and Nasser L. Hadipour*

Department of Chemistry, Tarbiat Modares University, P.O. Box 14115-175, Tehran, Iran

Received: January 16, 2006; In Final Form: April 3, 2006

A systematic computational study was carried out to characterize the ^{17}O , ^{14}N , and ^2H nuclear quadrupole resonance (NQR) parameters in the anhydrous and monohydrated cytosine crystalline structures. To include the hydrogen-bonding effects in the calculations, the most probable interacting molecules with the central molecule in the crystalline phase were considered in the pentameric clusters of both structures. To calculate the parameters, couples of the methods B3LYP and B3PW91 and the basis sets 6-311++G** and CC-pVTZ were employed. The mentioned methods calculated reliable values of ^{17}O , ^{14}N , and ^2H NQR tensors in the pentameric clusters, which are in good agreements with the experiment. The different influences of various hydrogen-bonding interactions types, $\text{N}-\text{H}\cdots\text{N}$, $\text{N}-\text{H}\cdots\text{O}$, and $\text{O}-\text{H}\cdots\text{O}$, were observed on the ^{17}O , ^{14}N , and ^2H NQR tensors. Lower values of quadrupole coupling constants and higher values of asymmetry parameters in the crystalline monohydrated cytosine indicate the presence of stronger hydrogen-bonding interactions in the monohydrated form rather than that of crystalline anhydrous cytosine.

1. Introduction

Hydrogen-bonding interactions (HBs) play a unique role in both chemical and biochemical systems. In a pioneering work, Watson and Crick indicated the importance of HBs between nucleobase pairs, AT and GC, in the stabilization of nucleic acid structures.¹ In addition, it was demonstrated that the nucleic acids are hydrated in living cells and also the three-dimensional (3D) structures of macromolecules are mainly due to these HBs among the nucleobases and water molecules.^{2–3} Therefore, the HBs in both nucleobase pairs and their hydrated forms have been previously studied employing various experimental and theoretical methods.^{4–7} Numerous studies have been also carried out to investigate the hydrogen-bonding capability of cytosine.^{8–11}

Since the characteristics of HBs are electrostatic, those techniques dealing with electron distributions around nuclei are preferred to detect and characterize the HB properties. Both X-ray and neutron diffraction studies were carried out to characterize the HBs of the crystalline cytosine structure.^{12–14} To have a better determination of the HB properties, NMR spectroscopy is among the most versatile techniques for the purpose.¹⁵ NMR parameters are very sensitive to the HBs and are useful elements in the study of hydrogen-bonded systems.^{16–17} Previously, Wu et al.¹⁸ and Hu et al.¹⁹ performed ^{17}O and ^{15}N solid-state NMR studies on cytosine, respectively. Although NMR parameters are very useful in determination of the HB properties, combination with the NQR parameters reveals a better interpretation of the observed results.²⁰

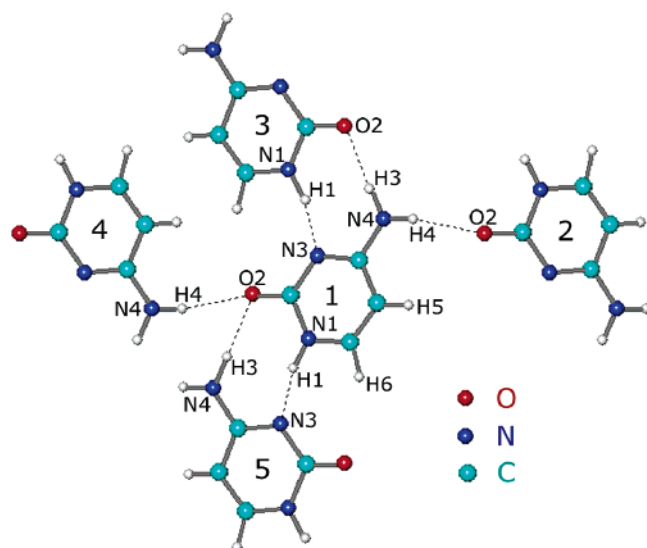
Nuclear quadrupole resonance (NQR) spectroscopy is an insightful technique to study various HB types.²¹ Nuclei with spin angular momentum, I , greater than one-half ($I > 1/2$), have the electric quadrupole moment, eQ , a characteristic which

interacts with the electric field gradient (EFG) at the sites of quadrupole nuclei.²² The quadrupole coupling constants, C_Q , and the asymmetry parameters, η_Q , are those experimentally measurable NQR parameters. C_Q indicates the interaction between EFG and eQ , whereas η_Q measures the deviation of EFG tensors from the axial symmetry. The experimental NQR parameters of cytosine were reported by Wu et al.¹⁸ and Rabbani et al.,²³ previously.

It is well-known that experimental studies are essential in the determination of HB properties, but combining them with systematic computational approaches leads to a better clarification of the observed results. Although numerous computational NMR and NQR studies were performed on cytosine so far,^{24–26} there is still a lack of a systematic study of cytosine in the literature. Recently, Ida et al.²⁷ carried out a systematic computational ^{17}O solid-state NMR study on crystalline uracil. In comparison with their earlier similar study on uracil,¹⁸ one can easily observe significant differences between the calculated parameters in the two levels of computations.

The present work includes a systematic computational ^{17}O , ^{14}N , and ^2H NQR study on the anhydrous and monohydrated cytosine crystalline structures. Considering the presence of HBs in the calculations, the most probable interacting molecules with the central molecule in the crystalline structures of anhydrous and monohydrated cytosine^{13,14} were considered in the pentameric clusters; see Charts 1 and 2 and Table 1 for details. Previous studies demonstrate the reproduction quality and reliability of calculated NQR parameters obtained from real crystalline structures.^{27–30} Density functional theory (DFT) was employed to calculate the ^{17}O , ^{14}N , and ^2H EFG tensors in this study. To have a comparison of HB influence on the various nuclei, EFG tensors were calculated for both forms of the monomer and pentameric clusters of the two structures. The EFG tensors converted into the NQR parameters, C_Q and η_Q , are exhibited in Tables 2–4.

* Author to whom correspondence should be addressed. E-mail: hadipour@modares.ac.ir or hadipour.n@gmail.com.

CHART 1: Intermolecular Hydrogen-Bonding Interactions of the Crystalline Anhydrous Cytosine

2. Computational Aspects

The DFT calculations were carried out by employing the Gaussian 98 package.³¹ The crystalline structures of anhydrous and monohydrated cytosine were available from X-ray and neutron diffraction studies, respectively.^{13–14} Since the positions of hydrogen atoms are not located accurately by X-ray diffraction, a geometry optimization of the just hydrogen atoms in the structure was needed. The optimization was performed at the B3LYP/6-311++G** level, where during this optimization the positions of the hydrogen atoms were allowed to fully relax while those of all other atoms remained frozen. For both anhydrous and monohydrated crystalline cytosine structures, pentameric clusters involving the most probable interacting molecules with the central molecule were created using coordinates transformation and were considered in the calculations; see Charts 1 and 2 and Table 1.

To calculate the ¹⁷O, ¹⁴N, and ²H EFG tensors in the principal axis system (PAS), two levels of DFT methods including B3LYP and B3PW91^{32–34} with the basis sets of 6-311++G** and CC-pVTZ were employed. To have a comparison among the capability of various nuclei and also each nucleus in contributing to HBs, all the calculations were performed for both forms of the monomer and the pentameric cluster of anhydrous and monohydrated cytosine; see Tables 2–4. Equation 1 is used to direct the relation of the calculated EFG tensors with experimental quadrupole coupling constants, C_Q . In this work, the reported standard Q values by Pyykkö³⁵ were used, $Q(^{17}\text{O}) = 25.58$ mb, $Q(^{14}\text{N}) = 20.44$ mb, and $Q(^2\text{H}) = 2.86$ mb

$$C_Q = e^2 Q q_{zz} h^{-1} \quad (1)$$

The asymmetry parameter, η_Q , which is an important NQR parameter in the measurement of the EFG tensors' deviation from axial symmetry, is obtained by eq 2

$$\eta_Q = |(q_{xx} - q_{yy})/q_{zz}| \quad (2)$$

3. Results and Discussion

The present work was carried out to investigate the HB effects on the ¹⁷O, ¹⁴N, and ²H EFG tensors of anhydrous and monohydrated cytosine crystalline structures. To this aim,

pentameric clusters of the two structures involving the most probable interacting molecules with the central molecule were created by transformation of the crystalline coordinates; see Charts 1 and 2 and Table 1 for details. The calculated EFG tensors were converted to the NQR parameters, C_Q , and η_Q , using eqs 1–2. The results for the monomer and the target molecule in pentameric clusters of anhydrous and monohydrated cytosine are summarized in Tables 2–4. By a quick look at the calculated results of the monomer and the target molecule in clusters, one can easily compare the capability of various nuclei in contributing to HBs. Indeed, more changes in each nucleus NQR parameter between the monomer and the target molecule in the cluster indicate its greater role among the other nuclei in contributing to HBs. The following text will discuss the ¹⁷O, ¹⁴N, and ²H NQR parameters in three sections, separately, where the results of B3PW91/cc-pVTZ are referred to.

3.1. ¹⁷O NQR Parameters. In this section, the calculated ¹⁷O quadrupole coupling constants, C_Q , and asymmetry parameters, η_Q , of anhydrous and monohydrated cytosine crystalline structures are discussed; see Table 2. A quick look at the results reveals the influence of HBs on the NQR parameters of oxygen. O2 contributes to two HB types, N–H...O and O–H...O, which both are strong ones. The following two subsections will discuss the properties of these HBs in the anhydrous and monohydrated cytosine crystalline structures, separately.

3.1.1. Crystalline Anhydrous Cytosine. In crystalline anhydrous cytosine, there are two possibilities for N–H...O HBs for O2: $r_{\text{O2}\cdots\text{N4-4}} = 2.98$ Å and $r_{\text{O2}\cdots\text{N4-5}} = 3.03$ Å. These HBs at O2 yield a significant reduction of the ¹⁷O quadrupole coupling constant from the monomer to the target molecule in the cluster: $\Delta C_Q(^{17}\text{O2}) = 1.79$ MHz. The experimental ¹⁷O quadrupole coupling constant of O2 was reported as 7.20 MHz by Wu et al.¹⁸ Among the different methods and basis sets, the result of B3PW91/cc-pVTZ has the least discrepancy from the experiment, $\Delta = 0.27$ MHz, when the standard $Q(^{17}\text{O})$ of 25.58 mb is used. However, through the use of the calibrated $Q(^{17}\text{O})$ of 23.94 mb,³⁶ B3LYP/6-311++G** also yields a reliable $C_Q(^{17}\text{O2})$ of 7.33 MHz, which differs from the experiment by just 0.13 MHz. Although this approach indicates the overestimating tendency of approximation methods in the ¹⁷O EFG tensors, the present work is based on using the standard values of Q for three reasons. First, this work aims to determine the capability of various nuclei in contributing to the HBs to obtain a better understanding of experimental results. So the discrepancies between the distinct values of calculated and experimental parameters were not important as much as the purpose of this work was concerned. Second, through the use of the standard Q , the efficiency of the various methods used in the calculation of EFG tensors were checked, and their overestimation tendencies were observed. Third, although the condition of crystalline anhydrous cytosine considered in the calculations was as close to the real crystalline structure as possible, there were still quite different conditions between computer and experiment. Thereby, the reasonable observed discrepancy between what is calculated in the computer and what is measured in the experiment is acceptable.

The significant reduction of $C_Q(^{17}\text{O2})$ from the monomer to the target molecule in cluster reveals the important role of O2 in contributing to the HBs in the crystalline cytosine. Besides, the increase of the asymmetry parameter is also significant from the monomer to the target molecule in the cluster: $\Delta\eta_Q(\text{O2}) = 0.47$. There is also a good agreement between the values of calculated and experimental $\eta_Q(\text{O2})$.

CHART 2: Intermolecular Hydrogen-Bonding Interactions of the Crystalline Monohydrated Cytosine

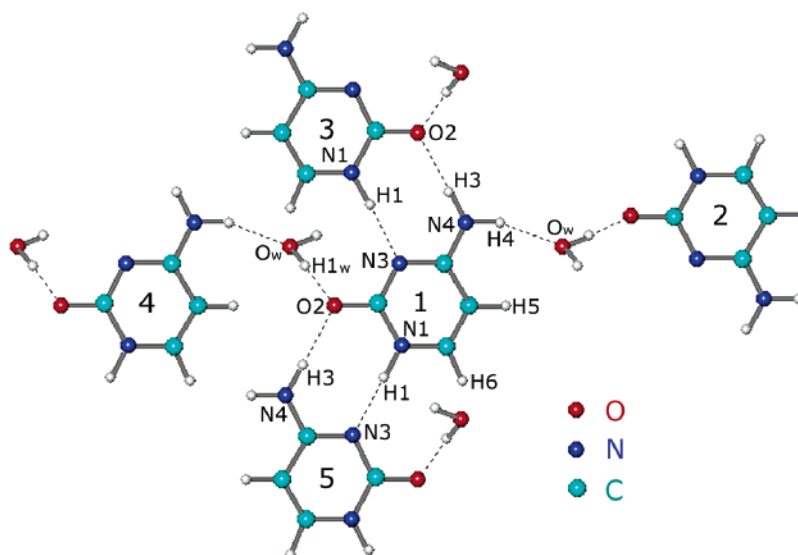


TABLE 1: Intermolecular Hydrogen-Bonding Distances

r^a	anhydrous cytosine ^b (Å)	monohydrated cytosine (Å)
N4...O2-2	2.98	
N4...O2-3	3.03	2.96
H4...O2-2	2.06	
H3...O2-3	2.02	1.94
N3...N1-3	2.84	2.95
N3...H1-3	1.87	1.91
O2...N4-4	2.98	
O2...N4-5	3.03	2.96
O2...H4-4	2.06	
O2...H3-5	2.02	1.94
N1...N3-5	2.84	2.95
H1...N3-5	1.87	1.91
N4...Ow-2		2.92
H4...Ow-2		1.95
O2...Ow		2.82
O2...H1w		1.86

^a For example, O2-2 is defined as O2 of molecule number 2 in Charts 1 and 2, etc. ^b After optimization of the hydrogens.

3.1.2. Crystalline Monohydrated Cytosine. In the crystalline monohydrated cytosine, the moiety of O2 in contributing to the HBs is somewhat different in comparison with what was mentioned above for the crystalline anhydrous cytosine. The two possibilities of O2 in contributing to the HBs in the monohydrated cluster are the N-H...O and O-H...O HB types: $r_{O2...N4-5} = 2.96$ Å and $r_{O2...Ow} = 2.82$ Å. Similar to the crystalline anhydrous cytosine, these HBs at O2 also reveal a significant reduction in the ^{17}O quadrupole coupling constant: $\Delta C_Q(^{17}\text{O2}) = 1.83$ MHz. In comparison with the anhydrous one, some trends are obtained. First, $C_Q(^{17}\text{O2})$ reduces a greater magnitude of 0.04 MHz in monohydrated rather than that of the anhydrous one. Second, the value of $C_Q(^{17}\text{O2})$ is 0.23 MHz smaller than that of the anhydrous one. As a result, in crystalline monohydrated cytosine, O2 contributes to stronger HBs.

The calculated $\eta_Q(\text{O2}) = 0.91$ is more significant than that of 0.77, which was calculated in crystalline anhydrous cytosine. Both the smaller value of $C_Q(^{17}\text{O2})$ and the larger value of $\eta_Q(\text{O2})$ in crystalline monohydrated cytosine rather than those of the crystalline anhydrous cytosine reveal greater influence of the HBs on the ^{17}O EFG tensors in this structure.

3.2. ^{14}N NQR Parameters. In this section, the discussion is focused on the calculated ^{14}N quadrupole coupling constants

and asymmetry parameters of crystalline anhydrous and monohydrated cytosine structures; see Table 3. Similar to the previous section, the calculated ^{14}N NQR parameters reveal the influence of HBs on the ^{14}N EFG tensors of the target molecule in both the crystalline anhydrous and the monohydrated cytosine clusters.

3.2.1. Crystalline Anhydrous Cytosine. Nitrogen nuclei contribute to two HB types in the crystalline anhydrous cytosine, N-H...N and N-H...O. As mentioned in the previous section, N-H...O HBs effects are significant on the ^{17}O EFG tensors. Similarly, N-H...O HBs also influence the ^{14}N EFG tensors. In the anhydrous cytosine cluster, N4 interacts with two neighboring oxygen atoms through N-H...O HBs: $r_{N4...O2-2} = 2.98$ Å and $r_{N4...O2-3} = 3.03$ Å. Because of the proper N...O distances, $C_Q(^{14}\text{N4})$ decreases by 1.20 MHz from the monomer to the target molecule in the cluster. $\eta_Q(\text{N4})$ also increases by 0.32 from the monomer to the cluster. These significant changes reveal the importance of the -NH₂ group in contributing to the strong HBs in the crystalline anhydrous cytosine. There is a good agreement between the calculated and the experimental values of $^{14}\text{N4}$ NQR parameters.

As mentioned above, the effects of N-H...O HBs are significant on the $^{14}\text{N4}$ EFG tensors. N1 and N3 contribute to another HB type, N-H...N: $r_{N...N} = 2.84$ Å. Because of the proper N...N distance, the effects of the N-H...O HBs on the N1 and N3 EFG tensors are also significant. $C_Q(^{14}\text{N1})$ decreases by 0.63 MHz, and $C_Q(^{14}\text{N3})$ decreases by 0.57 MHz from the monomer to the target molecule in the cluster. Although the magnitudes of these C_Q reductions are smaller than that of N4, the significant increases of 0.48 and 0.30 of $\eta_Q(\text{N1})$ and $\eta_Q(\text{N3})$, respectively, reveal their major role in contributing to the HBs. There is also a reasonable agreement between the calculated and the experimental N1 and N3 NQR parameters.

3.2.2. Crystalline Monohydrated Cytosine. In comparison with the crystalline anhydrous cytosine, N4 also has the capability of contributing to two N-H...O HBs in the crystalline monohydrated cytosine. However, one of these two oxygen atoms belongs to the water molecule: $r_{N4...O2-3} = 2.96$ Å and $r_{N4...Ow-4} = 2.92$ Å. The comparison of the two anhydrous and monohydrated structures reveals some trends. First, the N...O distances are shorter than those of anhydrous cytosine. Second, $C_Q(^{14}\text{N4})$ decreases by 0.26 MHz more than that of anhydrous cytosine, which reveals the greater HB effects on hydrated N4

TABLE 2: ^{17}O NQR Parameters of Anhydrous and Monohydrated Cytosine

nucleus	method	basis set	anhydrous cytosine				monohydrated cytosine				experiment ^b	
			C_Q (MHz)		η_Q		C_Q (MHz)		η_Q		C_Q (MHz)	η_Q
			monomer	cluster ^a	monomer	cluster ^a	monomer	cluster ^a	monomer	cluster ^a		
O2	B3LYP	6-311++G** cc-pVTZ	9.54	7.83	0.30	0.76	9.34	7.63	0.48	0.92	7.20	0.70
			9.36	7.56	0.26	0.73	9.17	7.34	0.44	0.90		
	B3PW91	6-311++G** cc-pVTZ	9.43	7.72	0.31	0.78	9.24	7.50	0.49	0.93		
			9.26	7.47	0.27	0.74	9.07	7.24	0.45	0.91		

^a The results were reported for the target molecule in the cluster. ^b The experimental values for anhydrous cytosine are from ref 18

TABLE 3: ^{14}N NQR Parameters of Anhydrous and Monohydrated Cytosine

nucleus	method	basis set	anhydrous cytosine				monohydrated cytosine				experiment ^b	
			C_Q (MHz)		η_Q		C_Q (MHz)		η_Q		C_Q (MHz)	η_Q
			monomer	cluster ^a	monomer	cluster ^a	monomer	cluster ^a	monomer	cluster ^a		
N1	B3LYP	6-311++G** cc-pVTZ	3.33	2.68	0.072	0.53	3.38	2.84	0.093	0.42	2.16	0.76
			3.15	2.49	0.083	0.57	3.20	2.64	0.12	0.44		
	B3PW91	6-311++G** cc-pVTZ	3.27	2.65	0.076	0.53	3.32	2.81	0.092	0.42		
			3.09	2.46	0.084	0.56	3.14	2.61	0.11	0.44		
N3	B3LYP	6-311++G** cc-pVTZ	3.75	3.22	0.54	0.83	3.71	2.98	0.57	0.96	3.41	0.20
			3.70	3.15	0.46	0.74	3.66	2.91	0.50	0.87		
	B3PW91	6-311++G** cc-pVTZ	3.68	3.13	0.55	0.86	3.64	2.89	0.60	0.99		
			3.64	3.07	0.47	0.77	3.60	2.83	0.51	0.89		
N4	B3LYP	6-311++G** cc-pVTZ	4.60	3.42	0.092	0.40	4.49	3.01	0.048	0.46	2.93	0.39
			4.55	3.29	0.075	0.40	4.42	2.90	0.031	0.46		
	B3PW91	6-311++G** cc-pVTZ	4.53	3.40	0.098	0.40	4.42	3.00	0.052	0.46		
			4.45	3.25	0.082	0.40	4.33	2.87	0.035	0.45		

^a The results were reported for the target molecule in the cluster. ^b The experimental values for anhydrous cytosine are from ref 23.

TABLE 4: ^2H NQR Parameters of Anhydrous and Monohydrated Cytosine

nucleus	method	basis set	anhydrous cytosine				monohydrated cytosine				experiment ^b	
			C_Q (kHz)		η_Q		C_Q (kHz)		η_Q		C_Q (kHz)	η_Q
			monomer	cluster ^a	monomer	cluster ^a	monomer	cluster ^a	monomer	cluster ^a		
H1	B3LYP	6-311++G** cc-pVTZ	275	242	0.15	0.21	226	191	0.17	0.22	162	0.23
			264	229	0.15	0.20	216	180	0.16	0.21		
	B3PW91	6-311++G** cc-pVTZ	276	244	0.15	0.20	227	192	0.17	0.22		
			267	231	0.15	0.19	218	182	0.16	0.21		
H3	B3LYP	6-311++G** cc-pVTZ	277	251	0.17	0.20	259	229	0.18	0.20	230	0.19
			265	238	0.17	0.19	247	217	0.17	0.19		
	B3PW91	6-311++G** cc-pVTZ	279	252	0.17	0.19	260	230	0.17	0.19		
			268	240	0.17	0.18	249	219	0.17	0.18		
H4	B3LYP	6-311++G** cc-pVTZ	287	268	0.19	0.18	264	238	0.21	0.19	236	0.18
			275	255	0.19	0.18	253	226	0.19	0.18		
	B3PW91	6-311++G** cc-pVTZ	289	269	0.19	0.18	266	239	0.20	0.18		
			277	258	0.18	0.17	256	228	0.19	0.17		

^a The results were reported for the target molecule in the cluster. ^b The experimental values for anhydrous cytosine are from ref 23.

EFG tensors. Third, the C_Q value of hydrated N4 is in the lower field rather than that of anhydrous cytosine. Fourth, $\eta_Q(\text{N4})$ increases more than that of anhydrous cytosine. These trends reveal stronger HB effects on the $-\text{NH}_2$ group due to monohydration in the crystalline cytosine.

Chart 2 shows that the monohydration does not have any direct influence on the other two nitrogen nuclei, N1 and N3, in the crystalline monohydrated cytosine. However, the $r_{\text{N} \cdots \text{N}}$ in the monohydrated structure is 0.11 Å longer than that of anhydrous one. From the monomer to the target molecule in the cluster, $C_Q(^{14}\text{N1})$ and $C_Q(^{14}\text{N3})$ decrease by 0.53 and 0.77 MHz, respectively. In contrast with the anhydrous cytosine, the

HBs influence the N3 EFG tensor more than that of N1 in the monohydrated structure.

From Table 1, it is noteworthy to mention some trends for monohydrated cytosine in comparison to the anhydrous one. First, $r_{\text{N1} \cdots \text{N3}-2}$ is longer than that of the anhydrous one, so a lesser influence of HBs is expected on the N1 EFG tensors. Second, although $r_{\text{N1} \cdots \text{Ow}-5} = 3.30$ Å is a proper distance of $\text{N}-\text{H} \cdots \text{O}$ HBs, $\angle \text{N1}-\text{H1} \cdots \text{Ow}-5 = 95.1^\circ$ disables this property. However, $r_{\text{N3} \cdots \text{Ow}} = 3.40$ Å and $\angle \text{N3} \cdots \text{H1}-\text{Ow} = 125.5^\circ$, so there is a greater probability for N3 to contribute to $\text{N3} \cdots \text{H1}-\text{Ow}$ HBs rather than N1. This trend is in agreement with the results of Table 3. $C_Q(^{14}\text{N3})$ decreases by 0.24 MHz

TABLE 5: BSSE of NQR Parameters (C_Q (MHz)) of Anhydrous and Monohydrated Cytosine

nucleus	anhydrous cytosine				monohydrated cytosine			
	B3LYP		B3PW91		B3LYP		B3PW91	
	6-311++G**	CC-pVTZ	6-311++G**	CC-pVTZ	6-311++G**	CC-pVTZ	6-311++G**	CC-pVTZ
O2	0.01	0.14	0.02	0.12	0.03	0.13	0.02	0.11
N1	0.01	0.03	0.01	0.02	0.01	0.03	0.01	0.02
N3	0.01	0.03	0.02	0.03	0.02	0.03	0.03	0.02
N4	0	0.06	0	0.05	0	0.03	0.01	0.03
H1	0	0	0.001	0.001	0	0	0	0
H3	0.001	0	0	0.001	0	0	0	0
H4	0	0.001	0.001	0	0.001	0	0	0.001

more than $C_Q(^{14}\text{N1})$ from the monomer to the target molecule in the cluster. Also, $\eta_Q(\text{N1}) = 0.44$ and $\eta_Q(\text{N3}) = 0.89$ reveal greater influence of HBs on N3 than N1.

3.3. ^2H NQR Parameters. By a first look at Charts 1 and 2, one may ask why the contributions of C–H to HBs were not considered. By a second look, some trends are observed to reply to this question. First, in the crystalline anhydrous cytosine, C–H5 and C–H6 have no electronegative nuclei in the neighborhood; see molecules number 3 and 4 in Chart 1. Second, in the crystalline monohydrated cytosine, although $r_{\text{H6}\cdots\text{Ow}-5} = 2.67 \text{ \AA}$, which is a rather proper HB distance, $\angle\text{C–H6}\cdots\text{Ow}-5 = 104.5^\circ$ and also the weak strength of the C–H \cdots O HB type refute the possibility of this HB for C–H6 and water. As a result, C5 and C6 have almost no chance of contributing to HBs. Since the EFG tensors are sensitive to the electron distribution around the nuclei, the NQR parameters of hydrogen nuclei are smaller than those of oxygen and nitrogen, which have lone pairs of electrons. Table 4 presents the calculated quadrupole coupling constants and asymmetry parameters of H1, H3, and H4.

H3 and H4 are those of the $-\text{NH}_2$ group that contribute to N–H \cdots O HBs. In the anhydrous cytosine, both H3 and H4 interact with the oxygen of neighboring cytosine molecules, but in the monohydrated cytosine, H4 interacts with the oxygen of a water molecule. As mentioned earlier about the influence of N \cdots O distance on the HB properties, different parameters were observed for H3 and H4.

H1, the hydrogen of N1, contributes to N–H \cdots N HBs with N3 where this HB type has been discussed in the previous section. From the monomer to the target molecule in both clusters, $C_Q(^2\text{H1})$ decreases more than $C_Q(^2\text{H3})$ and $C_Q(^2\text{H4})$. Hence, H2 EFG tensors feel more changes than those of H3 and H4 in both cytosine structures. The comparison between calculated and experimental results reveals a reasonable agreement between them.

3.4. Basis Set Superposition Error. Within this work, the basis set superposition error (BSSE) effects on the ^{17}O , ^{14}N , and ^2H EFG tensors were also studied via a counterpoise³⁷ method for the pentameric clusters; see Table 5. The results reveal that for O2 the BSSE is less than 0.12 MHz, and those of nitrogens were found to be less than 0.05 MHz. For hydrogens, there was almost no BSSE found in the two clusters. Since the values of the BSSE at the level of the present study are negligible, which is in agreement with the previous NMR study by Le and Oldfield,³⁸ the calculated EFG results were not corrected or modified. It is noteworthy that 6-311++G** almost shows no BSSE for the calculated EFG tensors.

4. Concluding Remarks

The preceding DFT study was carried out to investigate the HB effects on the ^{17}O , ^{14}N , and ^2H NQR parameters in the real crystalline anhydrous and monohydrated cytosine structures.

Considering this kind of clusters reveals reliable results that are in better agreement with the experiment. Nuclei in the anhydrous and monohydrated cytosine crystalline structures have different contributions to the HBs. Comparing the results of two structures reveals that the presence of a water molecule increases the strength of the HBs where the EFG tensors feel more changes. $C_Q(^{17}\text{O2})$ decreases by 0.2 MHz in the crystalline monohydrated cytosine. For N4, this change is more significant where $C_Q(^{14}\text{N4})$ decreases by 0.4 MHz more than that of the crystalline anhydrous cytosine. These different changes were also seen in other nuclei. The reasonable agreements between the calculated and the experimental NQR parameters reveal the reliability of the used methods, B3LYP and B3PW91, and basis sets, 6-311++G** and CC-pVTZ, in this study. And as a final note, 6-311++G** almost shows no BSSE for the calculated EFG tensors.

Acknowledgment. The authors gratefully thank Dr. Kamran Ahmadi for preparing the crystalline pentameric clusters of cytosine.

References and Notes

- (1) Watson, J. D.; Crick, F. H. *Nature* **1953**, *171*, 737.
- (2) Poltev, V. I.; Teplukhin, A. V.; Malenkov, G. G. *Int. J. Quantum Chem.* **1992**, *42*, 1488.
- (3) Kennard, O.; Hunter, W. N. *Angew. Chem., Int. Ed. Engl.* **1991**, *30*, 1254.
- (4) Sukhanov, O. S.; Shishkin, O. V.; Gorb, L.; Podolyan, Y.; Leszczynski, J. *J. Phys. Chem. B* **2003**, *107*, 2846.
- (5) Müller, A.; Frey, J. A.; Leutwyler, S. *J. Phys. Chem. A* **2005**, *109*, 5055.
- (6) Dąbkowska, I.; Gonzalez, H. V.; Jurečka, P.; Hobza, P. *J. Phys. Chem. A* **2005**, *109*, 1131.
- (7) Šponer, J.; Jurečka, P.; Hobza, P. *J. Am. Chem. Soc.* **2004**, *126*, 10142.
- (8) Sahu, P. K.; Mishra, R. K.; Lee, S.-L. *J. Phys. Chem. A* **2005**, *109*, 2887.
- (9) Hunter, K. C.; Rutledge, L. R.; Wetmore, S. D. *J. Phys. Chem. A* **2005**, *109*, 9554.
- (10) Kelly, R. E. A.; Lee, Y. J.; Kantorovich, L. N. *J. Phys. Chem. B* **2005**, *109*, 22045.
- (11) Gu, J.; Wang, J.; Leszczynski, J. *J. Am. Chem. Soc.* **2004**, *126*, 12651.
- (12) Barker, D. L.; Marsh, R. E. *Acta Crystallogr.* **1964**, *17*, 1581.
- (13) McClure, R. J.; Craven, B. M. *Acta Crystallogr., Sect. B* **1973**, *29*, 1234.
- (14) Weber, H. P.; Craven, B. M.; McMullan, R. K. *Acta Crystallogr., Sect. B* **1980**, *36*, 645.
- (15) Bovey, F. A. *Nuclear Magnetic Resonance Spectroscopy*; Academic Press: San Diego, 1988.
- (16) Brunner, E.; Sternberg, U. *Prog. Nucl. Magn. Reson. Spectrosc.* **1998**, *32*, 21.
- (17) Asakawa, N.; Kameda T.; Kuroki, S.; Kurosu, H.; Ando, S.; Ando, I.; Shoji, A. *Annu. Rep. NMR Spectrosc.* **1998**, *35*, 55.
- (18) Wu, G.; Dong, S.; Ida, R.; Reen, N. *J. Am. Chem. Soc.* **2002**, *124*, 1768.
- (19) Hu, J. Z.; Facelli, J. C.; Alderman, D. W.; Pugmire, R. J.; Grant, D. M. *J. Am. Chem. Soc.* **1998**, *120*, 9863.
- (20) Gervais, C.; Profeta, M.; Babonneau, F.; Pickard, C. J.; Mauri, F. *J. Phys. Chem. B* **2004**, *108*, 13249.

- (21) Das, T. P.; Han, E. L. *Nuclear Quadrupole Resonance Spectroscopy*; Academic Press: New York, 1958.
- (22) Cohen, M. H.; Rief, F. *Solid State Phys.* **1957**, *5*, 321.
- (23) Rabbani, S. R.; Edmonds, D. T.; Gosling, P. *J. Magn. Reson.* **1987**, *72*, 422.
- (24) Giessner-Prettre, C.; Pullman, B. *J. Am. Chem. Soc.* **1982**, *104*, 70.
- (25) Russo, N.; Sicilia, E.; Toscano, M.; Grand, A. *J. Mol. Struct.* **2001**, *563–564*, 125.
- (26) Latosińska, J. N.; Latosińska, M.; Koput, J. *J. Mol. Struct.* **2003**, *648*, 9.
- (27) Ida, R.; Clerk, M. D.; Wu, G. *J. Phys. Chem. A* **2006**, *110*, 1065.
- (28) Mirzaei, M.; Hadipour, N. L. *J. Phys. Chem. A* **2006**, *110*, 4833.
- (29) Elmi, F.; Hadipour, N. L. *J. Phys. Chem. A* **2005**, *109*, 1729.
- (30) Amini, S. K.; Hadipour, N. L.; Elmi, F. *Chem. Phys. Lett.* **2004**, *391*, 95.
- (31) Frisch, M. J.; Trucks, G. W.; Schlegel, H. B.; Scuseria, G. E.; Robb, M. A.; Cheeseman, J. R.; Zakrzewski, V. G.; Montgomery, G. A., Jr.; Stratmann, R. E.; Burant, J. C.; Dapprich, S.; Millam, J. M.; Daniels, A. D.; Kudin, K. N.; Strain, M. C.; Farkas, O.; Tomsai, J.; Barone, V.; Cossi, M.; Cammi, R.; Mennucci, B.; Pomelli, C.; Adamo, C.; Clifford, S.; Ochterski, J.; Petersson, G. A.; Ayala, P. Y.; Cui, Q.; Morokuma, K.; Malick, D. K.; Rabuck, A. D.; Raghavachari, K.; Foresman, J. B.; Cioslowski, J.; Ortiz, J. V.; Stefanov, B. B.; Liu, G.; Liashenko, A.; Piskorz, P.; Komaromi, I.; Comperts, R.; Martin, R. L.; Fox, D. J.; Keith, T.; Al-Laham, M. A.; Peng, C. Y.; Nanayakkara, A.; Gonzalez, C.; Challacombe, M.; Gill, P. M. W.; Johnson, B. G.; Chen, W.; Wong, M. W.; Andres, J. L.; Head-Gordon, M.; Replogle, E. S.; Pople, J. A. *Gaussian 98*, revision A.7; Gaussian, Inc.: Pittsburgh, PA, 1998.
- (32) Becke, A. D. *J. Chem. Phys.* **1993**, *98*, 5648.
- (33) Lee, C.; Yang, W.; Parr, R. G. *Phys. Rev. B* **1988**, *37*, 785.
- (34) Perdew, J. P.; Wang, Y. *Phys. Rev. B* **1992**, *45*, 13244.
- (35) Pyykkö, P. *Mol. Phys.* **2001**, *99*, 1617.
- (36) Dong, S.; Ida, R.; Wu, G. *J. Phys. Chem. A* **2000**, *104*, 11194.
- (37) Boys, S. F.; Bernardi, F. *Mol. Phys.* **1970**, *19*, 553.
- (38) Le, H.; Oldfield, E. *J. Phys. Chem.* **1996**, *100*, 16423.